

Molecular line observations of southern main-sequence stars with dust disks: α Ps A, β Pic, ϵ Eri and HR 4796 A*

Does the low gas content of the β Pic and ϵ Eri disks hint at the presence of planets?

R. Liseau

Stockholm Observatory, S-133 36 Saltsjöbaden, Sweden (rene@astro.su.se)

Received 21 January 1999 / Accepted 10 May 1999

Abstract. The results of molecular line observations with the 15 m SEST* of southern Vega-excess stars are presented. The stars α Ps A, ϵ Eri and HR 4796 A were observed in the CO (1–0) and (2–1) lines and β Pic was observed in the vibrational ground state of SiO, in the (2–1) and (5–4) transitions. In spite of considerably more sensitive observations than in previous attempts, none of these systems was detected with the SEST.

We use theoretical models of stellar atmospheres, of the structure and chemistry of interface regions (PDRs) and of molecular excitation in Keplerian disks of gas and dust to analyze these observational results. Among the observed objects, the K2 V star ϵ Eri appears particularly suitable and the analysis focusses on this system. A disk model with simple geometry is capable of explaining recent dust continuum observations. Applying this model to the associable molecular gas leads to the conclusion that it is most likely that the disk/ring around ϵ Eri is largely devoid of any gas ($m_{\text{gas}}/m_{\text{dust}}$ less than 10^{-3} of the interstellar value), presumably due to consumption during planetary system formation. We propose that ϵ Eri should be a prime candidate for searches for extrasolar planets.

In the β Pic disk, the gas content may be as low, or even lower, as for ϵ Eri which could be taken as indirect support of the suggested existence of a planetary system associated with this star.

Key words: stars: individual: ϵ Eri – stars: formation – stars: evolution – stars: circumstellar matter – stars: planetary systems – radio lines: stars

1. Introduction

Planet formation is thought to be complete by about 10 to 100 Myr (Lissauer 1993) and stars older than this could therefore potentially host planetary systems. Clues to the possible presence of planets in circumstellar disks around the stars include tidally deformed morphologies and/or small amounts of

remnant gas. Alternatively, the detection of resolved spectral lines from species spread out in the disks offers the opportunity to study the kinematics and the dynamical evolution of these disks. As typical temperatures in disks are relatively low, molecular rotational lines could be expected to provide a suitable tool, when heterodyne techniques with resolving powers of 10^6 or larger are exploited.

In this paper, we report millimetre line observations of four southern Vega-excess stars, which have recently been imaged in the infrared and/or the submillimetre. The Vega-phenomenon of main-sequence stars, discovered by IRAS (Auman et al. 1984), is discussed by Backman & Paresce (1993). Except for HR 4796 A, complementary and/or less sensitive searches had previously been reported (see: the references in Sect. 3). Observations, with varying success, of relatively large samples of (other) Vega-excess stars have been published by Zuckerman et al. (1995) and by Coulson et al. (1998).

The selected stars have ages in the range 10 to 1 000 Myr (Table 1) and may, in addition to their debris disks, possess planetary systems, either in the ‘making’ or already ‘finished’. The physical properties of the central stars and their disk systems are described in detail in the bibliography attached to Table 1, to which the reader is referred.

In Sects. 2 and 3, the observations and the results, respectively, are presented. In Sect. 4, these results are analyzed and discussed using theoretical models of stellar atmospheres, of the structure and chemistry of interface regions (PDRs: PhotoDominated Regions) and of molecular excitation in Keplerian disks of gas and dust, and the conclusions are briefly summarised in Sect. 5.

2. Observations

The observations were performed with the Swedish ESO Submillimetre Telescope (SEST) in August 1 and 2, 1998. The coordinates of the targets are listed in Table 1 and the observations were done simultaneously at two line frequencies. In both the 1 and 3 millimetre bands, SIS receivers were used as frontends. The backend was a 2×1 GHz multi-channel acousto-optical spectrometer (AOS), with 0.69 MHz wide channels and 1.4 MHz spectral resolution. The channel separation

Send offprint requests to: R. Liseau

* Based on observations collected with the Swedish ESO Submillimetre Telescope, SEST, in La Silla, Chile.

corresponds to, e.g., $\Delta v \sim 0.9 \text{ km s}^{-1}$ at 230 GHz (Table 2), and the observed band width is very much larger (more than $\times 100$) than the expected line width of the targets (of the order of 10 km s^{-1}) or any uncertainty as to their radial velocity (for the stars of Table 1, $0 < v_{\text{LSR}} < 6 \text{ km s}^{-1}$).

The half power beam width of the 15 m telescope is given in astronomical units (AU) in Table 2, for the differing distances and line frequencies. In order to achieve stable and flat baselines, dual wide-beam switching was exploited, with the beam-chop of $11'37$ in either positive or negative azimuth. The pointing of the telescope was regularly checked towards point sources, masing in the SiO ($v=1$, $J=2-1$) line, and determined to be better than $3''$ (rms).

The data are chopper-wheel calibrated in the T_{A}^* -scale (Ulich & Haas 1976). Typical noise levels are a few milli-Kelvin (rms) and the sensitivity to continuum emission is in the range 50 to 500 mJy in the 1 and 3 mm bands respectively (Table 2).

3. Results and comments on individual sources

In no case was either continuum or molecular line emission detected towards any of the stars and in Table 2, upper limits to the continuum flux density, S_{ν} in Jy, and to the line integral, $\int T_{\text{mb}} dv$ in K km s^{-1} , are listed. Below, a brief summary of previous and current results for the individual, alphabetically ordered, sources is provided.

α Ps A: Yamashita et al. (1993) have observed α Ps A in the CO(1–0) line with the 45 m Nobeyama telescope ($15''$ beam) and obtained a limiting line integral of $< 0.38 \text{ K km s}^{-1}$ in the T_{A}^* scale and for a 12 km s^{-1} interval. Using the 15 m JCMT ($14''$ beam), Dent et al. (1995) found for the CO(3–2) line $< 0.24 \text{ K km s}^{-1}$ in the T_{mb} scale and for the same velocity interval. The SEST data presented here are considerably more sensitive, and the CO(2–1) observation ($23''$ beam) is a new result ($< 0.05 \text{ K km s}^{-1}$ in the T_{mb} scale and integrated over 10 km s^{-1}).

β Pic: Savoldini & Galletta (1994) were first to use the SEST and to observe the star in the CO(1–0) line ($46''$ beam); they obtained $\int T_{\text{mb}} dv < 0.5 \text{ K km s}^{-1}$ for the velocity interval 12 km s^{-1} . Dent et al. (1995) found for the CO(2–1) line $< 0.072 \text{ K km s}^{-1}$ (JCMT, $21''$ beam) for the same velocity interval. CO(2–1) has also been observed with the SEST ($23''$ beam) by Liseau & Artymowicz (1998), which resulted in $< 0.06 \text{ K km s}^{-1}$, comparable to the result by Dent et al.. Here, renewed attempts have been made to detect gas phase SiO from the disk. The source was observed in two rotational transitions of the vibrational ground state, viz. in SiO(2–1) ($60''$ beam) and SiO(5–4) ($24''$ beam), and upper limits are $< 0.013 \text{ K km s}^{-1}$ and $< 0.011 \text{ K km s}^{-1}$, respectively (10 km s^{-1} integration). The new (2–1) measurement is three times more sensitive than that by Liseau & Artymowicz, whereas the SiO(5–4) observation represents a new result.

ϵ Eri: Yamashita et al. (1993) obtained a line integral $< 0.16 \text{ K km s}^{-1}$ in the T_{A}^* scale for the CO(1–0) transition ($15''$ beam). Dent et al. (1995) found for the CO(3–2) line ($14''$

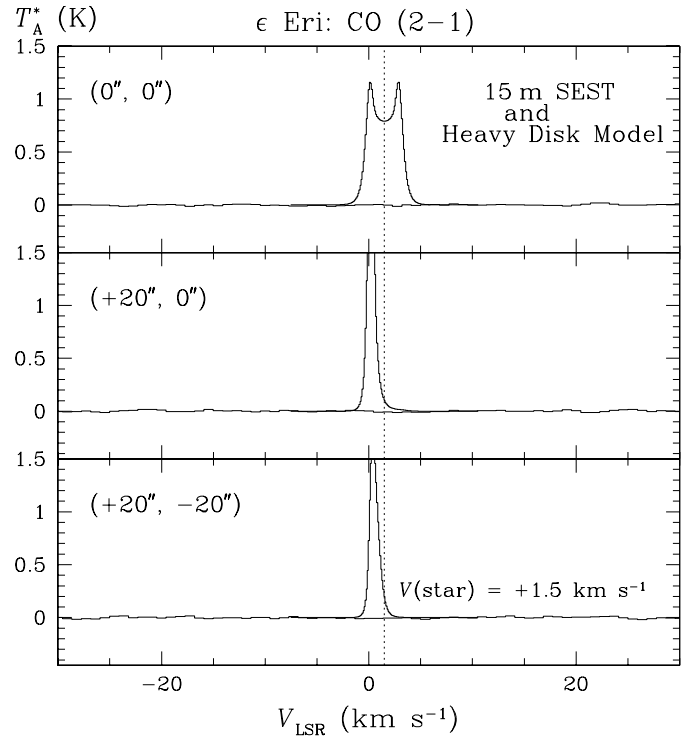


Fig. 1. SEST observations of ϵ Eri in the CO(2–1) line ($23''$ beam). Shown is only a small part of the observed spectra, which extend from -654 km s^{-1} to $+654 \text{ km s}^{-1}$ in LSR velocity. The displayed spectra refer to three positions (offsets are relative to the central star and $20'' = 64 \text{ AU}$) and are shown together with the expected line profiles from the *heavy* disk model (see: the text), where the sense of disk rotation has been assumed to be counter-clockwise

beam) $\int T_{\text{mb}} dv < 0.076 \text{ K km s}^{-1}$ for the same velocity interval, 12 km s^{-1} . Greaves et al. (1998) also used the JCMT, but in the CO(2–1) line ($21''$ beam) and towards a position offset by about $21''$ southeast of the star, and obtained $T_{\text{rms}} < 25 \text{ mK}$. Close to that location, viz. at offset $(\Delta \text{RA}, \Delta \text{Dec}) = (+19'', -7'')$ from the stellar position, their $850 \mu\text{m}$ image exhibits maximum brightness. The SEST observations were obtained towards the positions $(0'', 0'')$, $(+20'', 0'')$ and $(+20'', -20'')$ and are displayed in Fig. 1. The rms-noise in individual spectra is 7 mK for CO(2–1) and 15 mK for CO(1–0). In Table 2, the results from averaging these spectra are given.

HR 4796 A: The prime member of a triple system, HR 4796 A has not previously been searched for molecular line emission in the mm/submm regime and, hence, no comparisons can be made. The limits obtained at the SEST are $\int T_{\text{mb}} dv < 0.05$ and 0.03 K km s^{-1} , at the 1σ level, for CO(1–0) ($46''$ beam) and CO(2–1) ($23''$ beam), respectively.

4. Discussion

4.1. The A-type stars

4.1.1. α Ps A and HR 4796 A

An inherent difficulty, when observing inclined disk features with single dish antennae, is that of beam dilution. This problem

Table 1. Main sequence stars with circumstellar debris disks observed with the 15 m SEST

HR No.	Stellar Name	α (J2000)	δ (J2000)	Distance (pc)	Spectral Type	V_{hel} (km s ⁻¹)	Age (Myr)	References
1084	ϵ Eri	03 ^h 32 ^m 55 ^s .8	-09°27'30''	3.218 ± 0.009	K2 V	+16.7	500 – 10 ³	(1), (2), (3), (4)
2020	β Pic	05 47 17.1	-51 03 59	19.3 ± 0.2	A5 V	+21	10–100	(1), (2), (5), (6), (7)
4796 A	–	12 36 01.1	-39 52 11	67 ± 3	A0 V	+9.0 ± 1	8 ± 3	(1), (2), (8), (9), (10), (11)
8728	α Ps A	22 57 39.0	-29 37 20	7.69 ± 0.05	A3 V	+6.1	200 ± 100	(1), (2), (6), (7), (12), (13)

References: (1) Hipparcos Catalogue, 1997, ESA SP-1200; (2) Hipparcos Input Catalogue, 1992, ESA SP-1136; (3) Guenther 1987; (4) Greaves et al. 1998; (5) Crifo et al. 1997; (6) Holland et al. 1998; (7) Backman & Paresce 1993; (8) Stauffer et al. 1995; (9) Jayawardhana et al. 1998; (10) Koerner et al. 1998; (11) Jura et al. 1998; (12) Barrado y Navascués et al. 1997; (13) Barrado y Navascués 1998

Table 2. Molecular line observations of southern main sequence stars with particulate disks

Star	Transition ($v = 0$)	HPBW ^a (AU)	η_{mb} ^b (%)	η_{A} ^b (%)	Δv (km s ⁻¹)	τ_{atm}	T_{sys} (K)	t_{int} (s)	T_{rms} ^c (mK)	$S_{\nu}(\lambda_{\text{mm}})$ ^c (Jy)	I_{line} ^d (K km s ⁻¹)
ϵ Eri ^e	CO(2–1)	74	50	38	0.91	0.25	250	3 600	4.2	< 0.17 _(1.3 mm)	< 0.025
	CO(1–0)	145	70	58	1.80	0.30	420	3 600	8.1	< 0.22 _(2.6 mm)	< 0.049
β Pic	SiO(5–4)	463	50	40	0.97	< 0.03	200	10 000	1.8	< 0.07 _(1.4 mm)	< 0.011
	SiO(2–1)	1158	75	62	2.39	0.06	170	10 000	2.1	< 0.05 _(3.4 mm)	< 0.013
HR 4796 A	CO(2–1)	1541	50	38	0.91	0.16	260	3 000	5.1	< 0.21 _(1.3 mm)	< 0.031
	CO(1–0)	3015	70	58	1.80	0.24	370	3 000	8.0	< 0.22 _(2.6 mm)	< 0.048
α Ps A	CO(2–1)	177	50	38	0.91	0.22	280	1 200	8.0	< 0.33 _(1.3 mm)	< 0.048
	CO(1–0)	346	70	58	1.80	0.28	490	1 200	17.	< 0.46 _(2.6 mm)	< 0.10

^a Physical size of the half power beam width of the SEST at the distance of Table 1.

^b Main beam efficiency and aperture efficiency of the SEST, respectively, at the frequency of the transition.

^c T_{rms} is in the antenna temperature scale, T_{A}^* , and per velocity channel, Δv . S_{ν} is the corresponding flux density (1σ) at the wavelength λ in mm for η_{A} of this table.

^d The line integral, $I_{\text{line}} = \int T_{\text{mb}} dv$, is evaluated over an interval of 10 km s⁻¹ and has been estimated as $(T_{\text{rms}}/\eta_{\text{mb}})\Delta v\sqrt{N}$, where N is the number of velocity channels.

^e T_{rms} and S_{ν} for ϵ Eri are the averages of three different pointings (see the text).

may be particularly severe for the relatively distant HR 4796 A system, whose angular scale in the infrared is very much smaller than the SEST beam. Furthermore, HR 4796 A and α Ps A are of spectral type early-A and any gas present in the circumstellar disk would probably not be molecular, because the intense stellar UV field most likely dissociates any molecules more rapidly than they could form (Rentsch-Holm 1998, Rentsch-Holm et al. 1998).

4.1.2. β Pic

On the other hand, β Pic, being of type mid-A, could represent a borderline case, where the stellar field may not be able to destruct the CO gas in the disk (see the above references). The peculiar CO case of β Pic has been discussed in detail by Liseau & Artymowicz (1998) and will not be dwelled on further here. In that paper, we also discuss the observational consequences of a model of gas production through collisions of the silicate grains in the disk, which results in a significant abundance of silicon monoxide, SiO.¹ In light of this model, a possible interpretation of the observed upper limit to the SiO(5–4) line

is that the gas-to-dust mass ratio in the disk is lower than the average interstellar value by at least a factor of 10³, i.e. that the disk is virtually gas-free (see Fig. 2). If this assertion is correct, the total mass of the disk is appropriately estimated from dust continuum observations. Furthermore, the extremely low gas content of this disk could provide yet another piece of (indirect) evidence for the existence of planet(s) around β Pic (see Burrows et al. 1995 who discuss the warping of the disk).

4.2. The K-type star ϵ Eri

In contrast to the A stars, the well resolved disk/ring around the K2 star ϵ Eri ($T_{\text{eff}} \sim 4900$ K) presents a situation, where only the interstellar radiation field needs to be considered. This statement can be quantified in the following way: we use the model atmospheres by Kurucz (1992) to integrate the stellar surface flux over the wavelength interval 912–2067 Å, which corresponds to the energy interval of the G_0 scale (unity equals 1.6 10⁻³ erg cm⁻² s⁻¹, see: Tielens & Hollenbach 1985). The models for $T_{\text{eff}} = 4500$ K and 5000 K (with $\log g = 4.5$ and $\log(Z/Z_{\odot}) = 0.0$) yield distances from the central star at which

¹ Much of the presently observed dust in the β Pic disk is most probably not primordial but of secondary origin, as is the circumstellar

gas seen very close to the star (see, e.g., Artymowicz 1997 and Lagrange et al. 1995 and references therein).

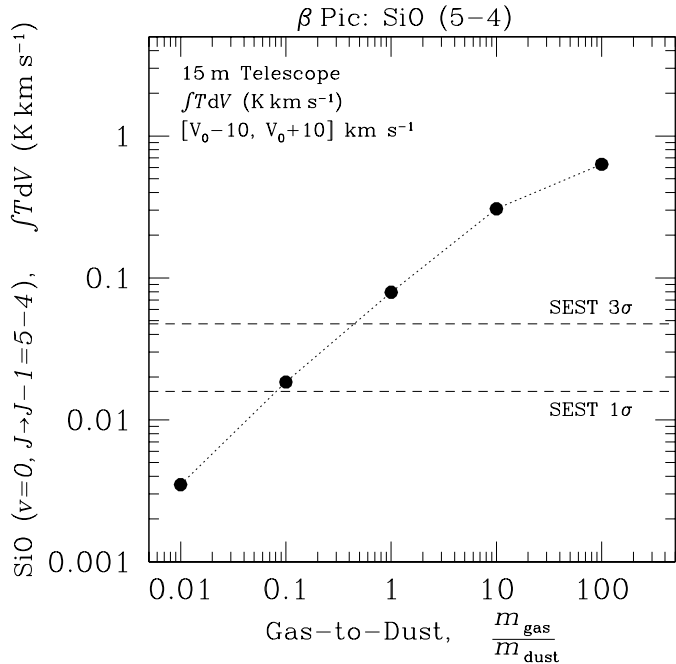


Fig. 2. The line integral of the SiO(5–4) transition ($\Delta v = 20 \text{ km s}^{-1}$) for various assumptions about the (total H_2) gas-to-dust mass ratio, $m_{\text{gas}}/m_{\text{dust}}$, in the β Pic disk. In the disk model considered, the average column density of gas phase SiO molecules is $N(\text{SiO}) = 1.5 \cdot 10^{12} \text{ cm}^{-2}$ (see: Liseau & Artymowicz 1998). The model values, shown by the filled dots, refer to observations with a 15 m telescope ($24''$ beam). The actual observation of β Pic with the SEST in the SiO(5–4) line resulted in an upper limit, which is indicated by the dashed lines corresponding to the 1σ and 3σ levels ($\Delta v = 20 \text{ km s}^{-1}$)

the diluted stellar UV field is comparable to the local interstellar field ($G_0 = 1$), viz. 3 AU and 28 AU respectively. These are obviously maximum radial distances, since the extinction by circumstellar grains has been neglected. Therefore, on the relevant disk scales of the order of 30 AU and larger (see: Greaves et al. 1998), the interstellar radiation field will dominate over that from ε Eri itself. Modelling of the circumstellar disk around this star becomes therefore relatively straightforward and, in the following, the discussion will focus on this particular system.

4.2.1. The dust belt/disk around ε Eri

The set of mm/submm continuum observations of ε Eri is somewhat incoherent (Table 3), which illustrates the difficulties of making absolute calibrations. Results obtained by Chini et al. (1990, 1991) are generally not in agreement with those published by others (see also the discussion by Zuckerman & Becklin 1993 and by Weintraub & Stern 1994), and flux discrepancies of the order of a factor of two or more are indicated. When trying to reproduce observed fluxes with models (see below), highest weight has been given to the observations by Greaves et al. (1998) though, since these are the most recent ones and also provide some spatial information. These authors also called attention to the close resemblance of the circumstellar dust around ε Eri to the Kuiper Belt of the solar system.

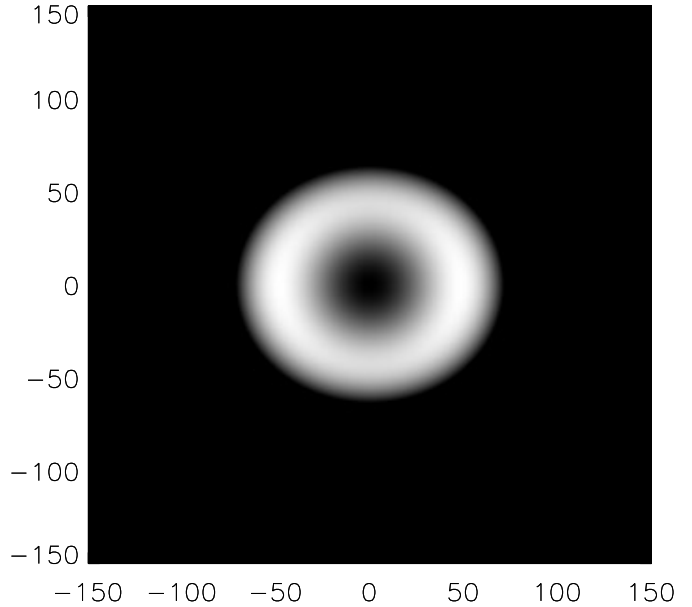


Fig. 3. 0.87 mm continuum image of the disk model for ε Eri, with the stellar position at the centre and units along the axes in AU. The disk midplane is assumed to be inclined by 65° with respect to the line of sight and the surface density to be proportional to the radial distance from the star. An $r^{-0.5}$ profile is used for the temperature. The mass of the dust disk is about $4 \cdot 10^{-3} M_{\oplus}$. The model has been convolved with a circular Gaussian of $\text{FWHM} = 15''$ ($\lesssim 50 \text{ AU}$) and displayed intensity levels correspond to about 0.7 to $1.0 I_{\text{max}}$ of the disk

Table 3. Model fluxes and mm/submm observations of ε Eri

theo λ (mm)	beam size ($''$)	theo S_ν (mJy)	obs S_ν (mJy)	obs λ (mm)	References
0.43	8	3	–	–	
0.43	70^\dagger	102	185 ± 103	0.45	(1)
0.87	15^\ddagger	4	3–5	0.85	(1)
0.87	70^\dagger	33	40 ± 3	0.85	(1)
0.87	9	1	35 ± 13	0.87	(2)
0.87	17	5	7.7 ± 7.7	0.80	(3)
1.30	12	1	7.5 ± 2.2	1.30	(2)
1.30	19	3	8.3 ± 6.4	1.30	(3)
1.30	24	5	24.2 ± 3.4	1.30	(4)

References: (1) Greaves et al. 1998; (2) Chini et al. 1990; (3) Zuckerman & Becklin 1993; (4) Chini et al. 1991

† In (1), the observations have been azimuthally averaged out to the radial distance $r \leq 35''$ from the stellar centre.

‡ Dito for $15''$ – $21''$ and estimated from Fig. 2 in (1).

We consider simple disk models, the details of which can be found in Liseau & Artymowicz (1998). The mass of the central star is assumed to be $0.8 M_{\odot}$ and the radius $0.8 R_{\odot}$. For the disk, power law temperature and surface density profiles are adopted, viz. $T(r) \propto r^p$ and $\Sigma(r) \propto r^q$ with $p = -0.5$ and $q = 1$. Inner and outer radii are 4 AU and 85 AU, respectively, and $T(r_{\text{in}}) = 135 \text{ K}$ (Yamashita et al. 1993). Consequently, the

temperature at the outer ‘edge’ of the disk is $T(r_{\text{out}}) \lesssim 30$ K. The disk midplane is inclined with respect to the line of sight by 65° (Greaves et al. 1998). The gas-to-dust mass ratio, $m_{\text{gas}}/m_{\text{dust}}$, is used as a free parameter and assumed constant throughout the disk. The high value of the dust opacity used by Greaves et al. (1998; see also: Zuckerman & Becklin 1993) was adopted, viz. $\kappa_{\nu}(850 \mu\text{m}) = 1.7 \text{ cm}^2 \text{ g}^{-1}$, yielding minimum estimates of the disk masses. The possible, or even likely, existence of pebbles, boulders, planetesimals etc. in the disk is not accounted for. Blackbody emissivity of the relatively large grains is suggested by the mm/submm continuum observations, so that $\beta = 0$ when $\kappa_{\nu} \propto \nu^{\beta}$.

From the fitting of the continuum observations (Table 3), the *dust* mass of the disk is found to be $4.3 \cdot 10^{-3} M_{\oplus}$ (see also: Greaves et al. 1998). There are discrete features in the observed $850 \mu\text{m}$ image by these authors, but the general appearance is that of a ring or belt, with some non-zero flux near the centre, however. This doughnut shape is reasonably well reproduced by the model (although it is not), as can be seen in Fig. 3, where no attempt has been made to ‘tune’ the model to perfection, by, e.g., fiddling around with the density distribution and/or by including clumps at appropriate places.

4.2.2. The amount of gas in the ε Eri disk: heavy molecular disk

The *heavy* disk hypothesis assumes a ‘normal’ gas-to-dust mass ratio of 100, which results in a total disk mass² of $0.44 M_{\oplus}$ ($1.3 \cdot 10^{-6} M_{\odot}$) and an average density of $n(\text{H}_2) = 1.5 \cdot 10^6 \text{ cm}^{-3}$. PDR model computations using CLOUDY (Ferland et al. 1998; for details, see: Liseau et al. 1999) show that, for most parts of the disk, vertical column densities are also sufficiently high to shield both H_2 and CO against photodissociation by the local UV field, $G_0 = 1$. A value of, e.g., $G_0 = 10$, which would more than well compensate for the previously ignored slight chromospheric excess (see: Wu et al. 1983 for the UV spectrum of the star), does basically not alter this conclusion. Therefore, any gas in such a heavy disk could be expected to be largely molecular and, specifically, CO not to be dissociated.

For the interstellar value of the relative abundance of CO, $X(\text{CO}) = n(\text{CO})/n(\text{H}_2) = 10^{-4}$, the predicted intensity of the CO (2–1) line would be 7.6 K km s^{-1} (integrated over $\Delta V = 10 \text{ km s}^{-1}$). This is larger by a factor of 300 than what has been observed (Table 2).

Alternatively, for the ratio $m_{\text{gas}}/m_{\text{dust}} = 100$, the CO (2–1) data could also be interpreted to imply $X(\text{CO}) \lesssim 2 \cdot 10^{-7}$. A tentative reason for such a dramatic reduction of the gas phase CO abundance could be freeze-out of CO onto the grains. However, model disk temperatures are considerably higher (above 30 K) than the sublimation temperature of CO ice (~ 17 K; van Dishoeck et al. 1993), and there is no immediately good reason,

why CO should be largely underabundant. We therefore seek an alternate explanation in the next section.

4.2.3. The amount of gas in the ε Eri disk: light dust disk

The simplest, and internally most consistent, explanation is that the disk is *light*, i.e. essentially gas-free. Specifically, and keeping with $X(\text{CO}) = 10^{-4}$, a model with $m_{\text{gas}}/m_{\text{dust}} \leq 0.1$ is compatible with the observational limit on the CO emission. This would imply a strict limit to the *average* CO column density through the disk of $N(\text{CO}) < 10^{13} \text{ cm}^{-2}$. Obviously, the mass of the disk is in this case completely dominated by the dust component ($M_{\text{disk}} \sim 4 \cdot 10^{-3} M_{\oplus}$). The average volume density of hydrogen gas is $n(\text{H} + 2 \text{H}_2) \leq 3 \cdot 10^3 \text{ cm}^{-3}$.

For such a low gas density, one might speculate that the local interstellar UV field could seriously affect the chemistry in the disk. In fact, PDR model calculations show that both hydrogen and carbon (as well as oxygen) are essentially atomic throughout the disk ($\text{H}_2/\text{H} \sim 10^{-2}$, $\text{CO}/\text{C} \sim 10^{-3}$). Therefore, and consistently, detectable molecular line emission is not expected from the *light* disk model. Although the cooling of the disk gas would be totally dominated by the [C II] $158 \mu\text{m}$ line (solar abundances are assumed), predicted intensities ($\lesssim 10^{-8} \text{ erg cm}^{-2} \text{ s}^{-1} \text{ sr}^{-1}$ for $n(\text{H}) = 3 \cdot 10^3 \text{ cm}^{-3}$) are far below current detection capabilities.

4.2.4. Substellar mass companions

The 1 Gyr old star ε Eri seems thus to be surrounded by material, which presumably represents the remnants of a rotating, once gas-rich, accretion disk (cf. Guenther 1987 for a discussion of the age of the star). Much of the initially present gas may have ended up in planets, which may be found within the inner 30 AU around the star (see also Greaves et al. 1998; the planetary hypothesis has also been put forward by Das & Backman 1992, although with few details regarding the supporting evidence). On the basis of astrometric measurements, van de Kamp (1974) proposed that ε Eri has a companion of substellar mass at $\lesssim 2''$ (7 AU) separation. Recent HST images by Krist et al. (1997) seemed not to reveal this companion, since no mentioning was made by the authors. From the single body analysis by van de Kamp, the mass would then correspond to his ‘infinite magnitude’ solution, i.e. of the order of $6 M_{\text{Jupiter}}$. In summary, it seems that ε Eri ought to be a prime candidate for searches for nearby extrasolar planets.

5. Conclusions

The main conclusions from this work can be summarized as follows:

- SEST observations of the disks around the southern Vega-excess stars α Ps A (Fomalhaut), ε Eri and HR 4796 A have not been successful to detect emission in rotational lines of CO or, towards β Pic, of SiO.
- The non-detections of the early A-type stars α Ps A and HR 4796 A could in principle be due to photodissociation

² This value depends, among other things, on the assumed dust opacity. Were that much lower, say $0.1 \text{ cm}^2 \text{ g}^{-1}$, the minimum mass of the disk would increase accordingly (to $7.4 M_{\oplus}$).

of the molecules (Rentsch-Holm 1998) or, simply, be due to the absence of gas, perhaps because of planet formation, in the circumstellar disks. However, the precise status remains inconclusive.

- Physical conditions around the K 2 star ε Eri appear more favourable for theoretical modelling, which leads to the conclusion that circumstellar gas is probably not present at levels higher than 10^{-1} times the dust content of the disk. We propose that much of the primordial disk gas has ended up in a planetary system and that searches for that should be intensified.
- The non-detection of the SiO (5–4) line towards β Pic may indicate that the gas-to-dust mass ratio of the β Pic disk is at least 10^3 times smaller than the average value of the interstellar medium. As for ε Eri, this may be indirect evidence for the presence of a planetary system around the star.

Acknowledgements. B. Larsson is thanked for his assistance with the IDL routines. This research has been supported by the Swedish Natural Science Research Council (NFR).

References

- Artymowicz P., 1997, *Ann. Rev. Earth Planet. Sci.* 25, 175
 Auman H.H., Gillet F.C., Beichman F.C., et al., 1984, *ApJ* 278, L 23
 Backman D.E., Paresce F., 1993, In: Levy E.H., Lunine J.I. (eds.) *Protostars & Planets III*, University of Arizona Press, p. 1253
 Barrado y Navascués D., 1998, *A&A* 339, 831
 Barrado y Navascués D., Stauffer J.R., Hartmann L., Balachandran S.C., 1997, *ApJ* 475, 313
 Burrows C.J., Krist J.E., Stapelfeldt K.R., WFPC2 Investigation Definition Team, 1995, *A&AS* 187, 32.05
 Chini R., Krügel E., Kreysa E., 1990, *A&A* 227, L 5
 Chini R., Krügel E., Shustov B., Tutukov A., Kreysa E., 1991, *A&A* 252, 220
 Coulson I.M., Walther D.M., Dent W.R.F., 1998, *MNRAS* 296, 934
 Crifo F., Vidal-Madjar A., Lallement R., Ferlet R., Gerbaldi M., 1997, *A&A* 320, L 29
 Das S.R., Backman D.E., 1992, *A&AS* 181, 68.04
 Dent W.R.F., Greaves J.S., Mannings V., Coulson I.M., Walther D.M., 1995, *MNRAS* 277, L 25
 Ferland G.J., Korista K.T., Verner D.A., et al., 1998, *PASP* 110, 761
 Greaves J.S., Holland W.S., Moriarty-Schieven G., et al., 1998, *ApJ* 506, L 133
 Guenther D.B., 1987, *ApJ* 312, 211
 Holland W.S., Greaves J.S., Zuckerman B., et al., 1998, *Nat* 329, 788
 Jayawardhana R., Fisher S., Hartmann L., et al., 1998, *ApJ* 503, L 79
 Jura M., Malkan M., White R., et al., 1998, *ApJ* 505, 897
 Koerner D.W., Ressler M.E., Werner M.W., Backman D.E., 1998, *ApJ* 503, L 83
 Krist J.E., Burrows C.J., Stapelfeldt K.R., WFPC2 ID Team, 1997, *A&AS* 191, 05.14
 Kurucz R.L., 1992, In: Barbuy B., Renzini A. (eds.) *The Stellar Populations of Galaxies*. IAU Symp. 149, p. 225
 Lagrange A.M., Vidal-Madjar, A., Deleuil M., et al., 1995, *A&A* 296, 499
 Liseau R., Artymowicz P., 1998, *A&A* 334, 935
 Liseau R., White G.J., Larsson B., et al., 1999, *A&A* 344, 342
 Lissauer J.J., 1993, *ARA&A* 31, 129
 Rentsch-Holm I., 1998, Ph.D. Thesis, Kiel University
 Rentsch-Holm I., Holweger H., Bertoldi F., 1998, In: Yun J.L., Liseau R. (eds.) *Star Formation with the Infrared Space Observatory*. ASP Conf. Ser. 132, p. 275
 Savoldini M., Galletta G., 1994, *A&A* 285, 467
 Stauffer J.R., Hartmann L.W., Barrado y Navascués D., 1995, *ApJ* 454, 910
 Tielens A.G.G.M., Hollenbach D.J., 1985, *ApJ* 291, 722
 Ulich B.L., Haas R.W., 1976, *ApJS* 30, 247
 van de Kamp P., 1974, *AJ* 79, 491
 van Dishoeck E.F., Blake G.A., Draine B.T., Lunine J.I., 1993, In: Levy E.H., Lunine J.I. (eds.) *Protostars and Planets III*, Univ. Arizona Press, Tucson, p. 163
 Weintraub D.A., Stern S.A., 1994, *AJ* 108, 701
 Wu C.-C., Ake T.B., Boggess A., et al., 1983, *IUE NASA Newsletter* 22
 Yamashita T., Handa T., Omodaka T., et al., 1993, *ApJ* 402, L 65
 Zuckerman B., Becklin E.E., 1993, *ApJ* 414, 793
 Zuckerman B., Forveille T., Kastner J.H., 1995, *Nat* 373, 494